Supplementary Tables and Figures

Table S1. Source-wise emissions of NO_x, CO and NMVOCs for the year 2000 implemented in the ACCMIP models. Anthropogenic emissions include emissions from anthropogenic sources, biomass burning, shipping, and aircraft (for NO_x only). A cell with n/a means that the quantity was not available.

	NO_x (Tg N yr^{-1})				CO (Tg CO yr^{-1})				NMVOCs (Tg C yr^{-1})			
Models	**Anthro**	**Lightning**	**Soil**	**Total**	**Anthro**	**Biogenic**	**Ocean**	**Total**	**Anthro**	**Biogenic**	**Ocean**	**Total**
CESM-CAM-superfast	38.8	4.2	4.9	47.9	1073	176[c]	-	1249	0	429	0	429
CICERO-OsloCTM2	37.7	5.0	8.0	50.7	1070	160	20	1250	65	396	0	462
CMAM	37.7	3.8	9.3	50.8	1073	410	20	1503	0	0	0	0
EMAC	38.0	5.7	3.6	47.3	1065	113[c]	-	1178	161	419	0	580
GEOSCCM	33.0[a]	5.0	7.2	45.2	1071	166	0	1237	72	556	0	628
GFDL-AM3	38.3	4.4	3.6	46.3	1071	159	20	1250	91	737	4	833
GISS-E2-R	38.2	7.7	2.7	48.6	1072	0	0	1072	78	753	0	830
GISS-E2-R-TOMAS	38.3	7.2	2.7	48.2	1069	0	0	1069	77	764	0	841
HadGEM2	37.3	1.2	5.6	44.1	1068	475	45	1588	104	0	0	104
LMDzORINCA	38.2	5.9	8.7	52.8	1068	0	20	1088	122	535	0	657
MIROC-CHEM	n/a	9.7	n/a	47.8	n/a	0	n/a	1068	212	624	0	836
MOCAGE	38.2	5.2	4.5	47.9	609	560[c]	-	1170	98	962[c]	-	1060
NCAR-CAM3.5	39.1	4.1	4.9	48.0	1073	176[c]	-	1249	114	554	0	668
STOC-HadAM3	38.2	7.2	5.6	50.9	1068	75	25	1168	136	576	0	712
TM5[b]	38.5	6.0	5.0	49.5	1085	76	20	1181	113	506	3	622
UM-CAM	36.4	5.1	7.0	48.5	1053	100[c]	-	1153	149	374	0	523

[a] Shipping emissions were not included in the model

[b] Base year is 2006

[c] Oceanic emission totals are included

Table S2. The expression for temperature-dependent rate coefficient (k_{CH4+OH}) for methane oxidation implemented in the models and its global annual mean value for 1850, 1980, and 2000 time-slices. Multi-model mean (MMM) with standard deviation (STD) and coefficient of variation (CV) are shown in the last two rows.

		k_{CH4+OH} (10^{-5} cm^3 molec^{-1} s^{-1})		
Models	**Expression for k_{CH4+OH}**	**1850**	**1980**	**2000**
CESM-CAM-superfast	2.45×10^{-12} exp(-1775/T)	3.046	3.101	3.144
CICERO-OsloCTM2	2.45×10^{-12} exp(-1775/T)	3.085	3.085	3.085
CMAM	2.45×10^{-12} exp(-1775/T)	3.036	3.075	3.120
EMAC	$1.85\times10^{-12} * T^{2.82}$exp(-987/T)	3.037	3.057	3.099
GEOSCCM	$2.80\times10^{-14} * T^{0.667}$exp(-1575/T)	3.062	3.092	3.130
GFDL-AM3	2.45×10^{-12} exp(-1775/T)	2.999	2.999	3.038
GISS-E2-R	2.45×10^{-12} exp(-1775/T)	3.016	3.050	3.083
GISS-E2-R-TOMAS	2.45×10^{-12} exp(-1775/T)	2.996	3.040	3.083
HadGEM2	2.45×10^{-12} exp(-1775/T)	3.022	3.026	3.061
LMDzORINCA	2.45×10^{-12} exp(-1775/T)	2.997	3.025	3.053
MIROC-CHEM	2.45×10^{-12} exp(-1775/T)	2.937	2.991	2.991
MOCAGE	2.45×10^{-12} exp(-1775/T)	2.966	3.004	3.027
NCAR-CAM3.5	2.45×10^{-12} exp(-1775/T)	2.975	3.002	3.052
STOC-HadAM3	2.45×10^{-12} exp(-1775/T)	2.964	2.980	3.011
TM5	2.45×10^{-12} exp(-1775/T)	3.098	***	3.098
UM-CAM	1.85×10^{-12} exp(-1690/T)	3.039	3.050	3.083
MMM±STD		3.02±0.04	3.04±0.04	3.07±0.04
CV (%)		1.5	1.3	1.4

Table S3. Methane lifetime calculated as global burden of methane divided by tropospheric methane loss flux with the tropopause defined as air with ozone concentrations less than or equal to 150 ppbv in the 1850 time-slice simulation. Multi-model mean (MMM) with standard deviation (STD) and coefficient of variation (CV) are shown in the last two rows.

	τ_{CH4} (years)		
Models	**1850**	**1980**	**2000**
CESM-CAM-superfast	9.2	8.7	8.3
CICERO-OsloCTM2	9.0	10.0	9.9
CMAM	8.7	9.6	9.4
EMAC	8.8	9.4	9.0
GEOSCCM	8.5	9.6	9.5
GFDL-AM3	8.8	9.6	9.3
GISS-E2-R	11.8	11.3	10.6
GISS-E2-R-TOMAS	10.3	9.8	9.1
HadGEM2	11.5	12.0	11.5
LMDzORINCA	10.0	10.6	10.4
MIROC-CHEM	n/a	n/a	8.7
MOCAGE	8.1	7.5	7.0
NCAR-CAM3.5	10.6	9.8	9.1
STOC-HadAM3	9.6	9.5	9.1
UM-CAM	14.9	14.7	13.9
MMM±STD	10.0±1.8	10.2±1.7	9.7±1.6
CV (%)	18.0	17.0	16.0

Table S4. Ratio of global total CO, NOx and NMVOC emissions in the present day (2000) to those in preindustrial (1850) in the models.

	2000/1850 Global Total Emissions		
Models	**CO**	**NOx**	**NMVOCs**
CESM-CAM-superfast	2.21	3.85	1.00
CICERO-OsloCTM2	2.21	2.74	1.12
CMAM	1.82	2.77	-
EMAC	2.38	3.33	1.29
GEOSCCM	2.34	2.61	1.27
GFDL-AM3	2.20	3.36	1.09
GISS-E2-R	2.77	3.07	1.15
GISS-E2-R-TOMAS	2.77	3.20	1.03
HadGEM2	1.75	3.77	1.52
LMDzORINCA	2.69	3.25	1.18
MIROC-CHEM	2.78	3.27	1.15
MOCAGE	2.40	3.22	1.12
NCAR-CAM3.5	2.21	3.99	1.16
STOC-HadAM3	2.41	2.83	1.26
TM5	2.45	3.02	1.16
UM-CAM	2.39	2.83	1.25
MMM±STD	2.36±0.30	3.19±0.41	1.18±0.13

Figure S1. Regional annual mean airmass-weighted OH concentrations ($x10^5$ molecule cm^{-3}) for 2000 simulated by the models in the atmospheric subdomains recommended by Lawrence et al. (2001). Global mean tropospheric OH concentrations (Glob) and the inter-hemispheric ratio (N/S) are shown in the topmost row of each plot.

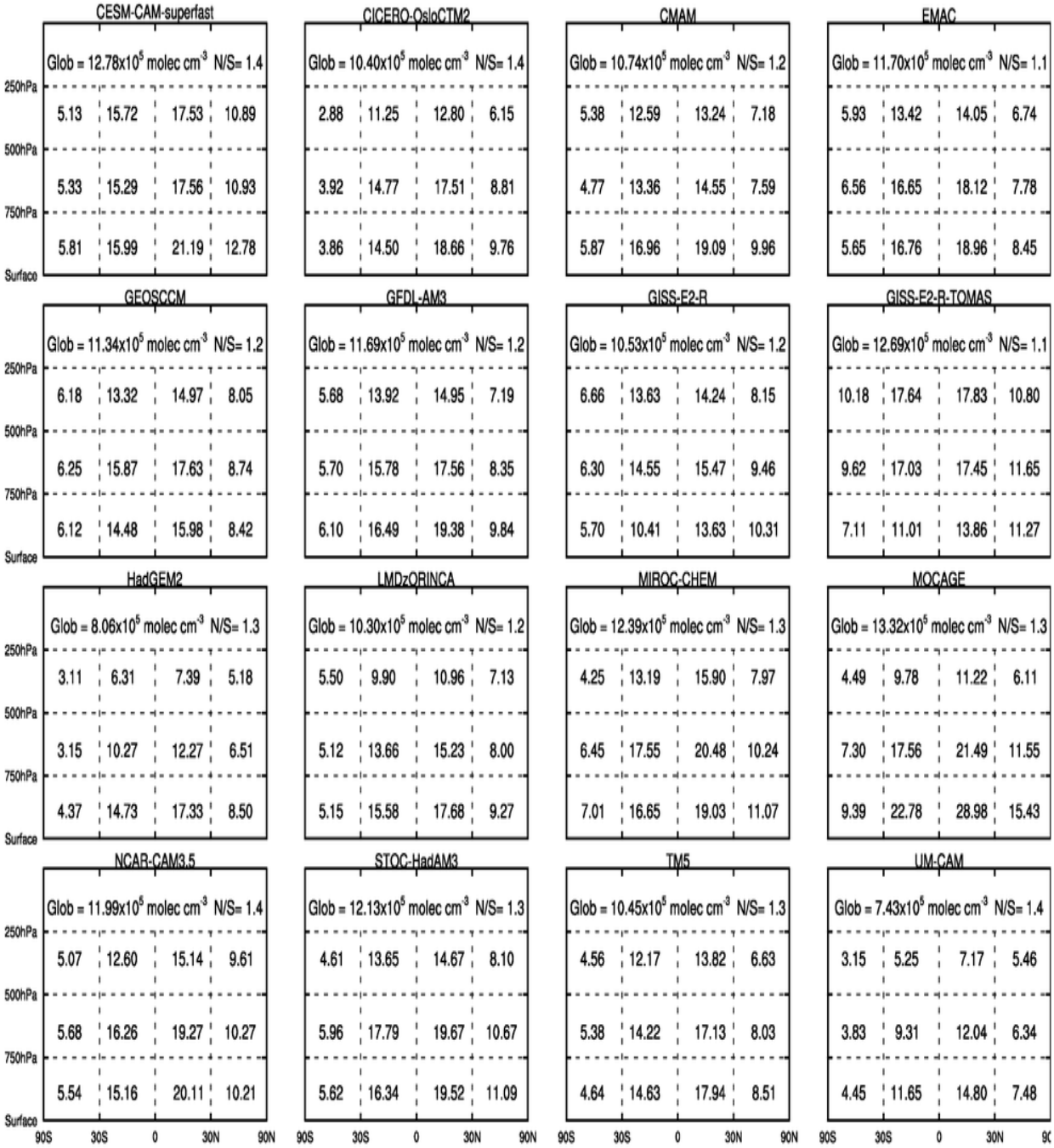

Figure S2. Annual cycle of total column ozone biases for 2000 against satellite measurements from the merged Total Ozone Mapping Spectrometer/solar backscatter ultraviolet (TOMS/SBUV) data averaged over the 1996-2005 time period. ENS refers to multi-model mean bias against TOMS/SBUV data.

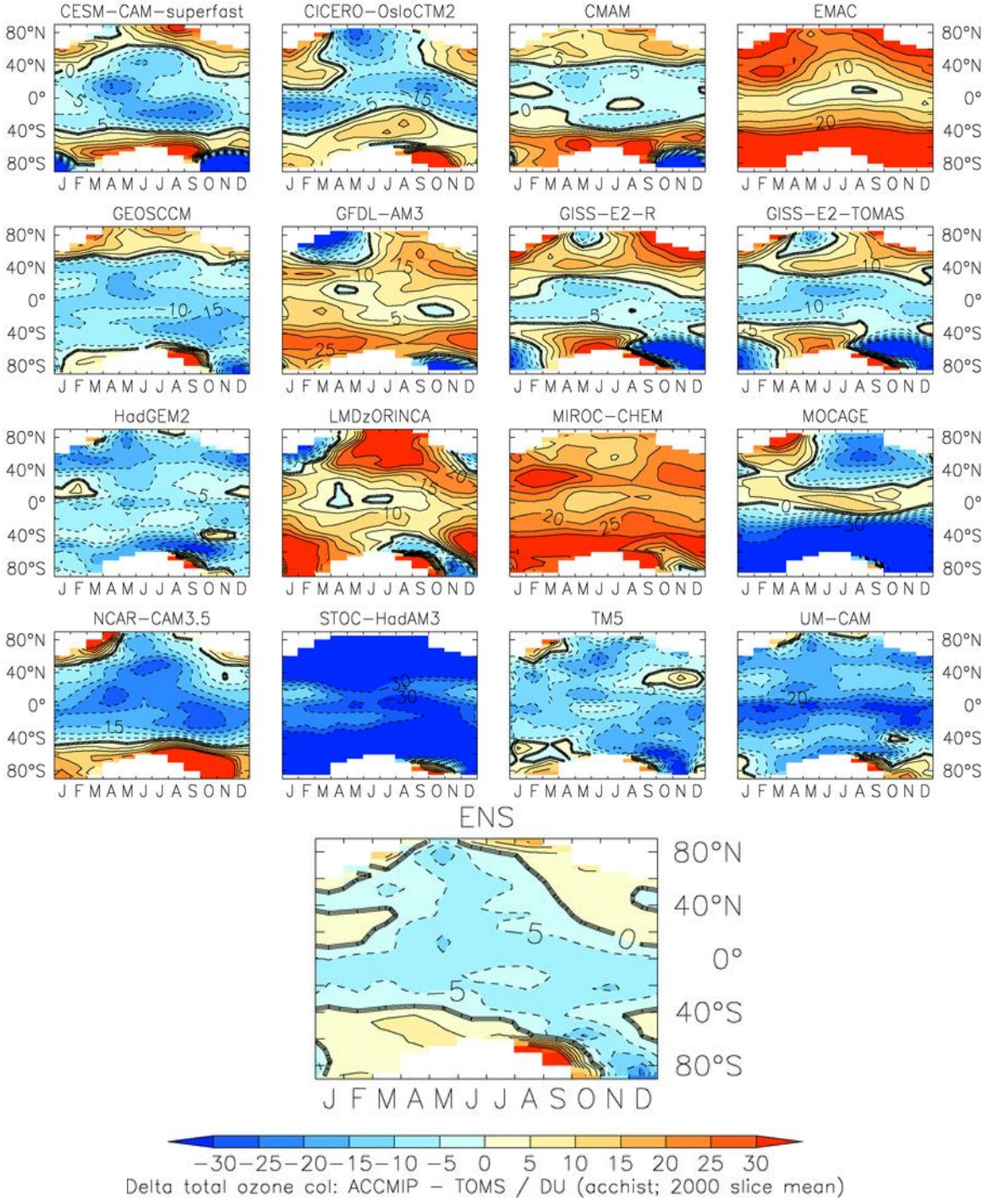

Figure S3. Annual average difference between model CO for 2000 time-slice and average 2000-2006 MOPITT (Model-MOPITT) at 500 hPa for individual models. Each model was convolved with the MOPITT operator (a priori and averaging kernels) before taking the difference.

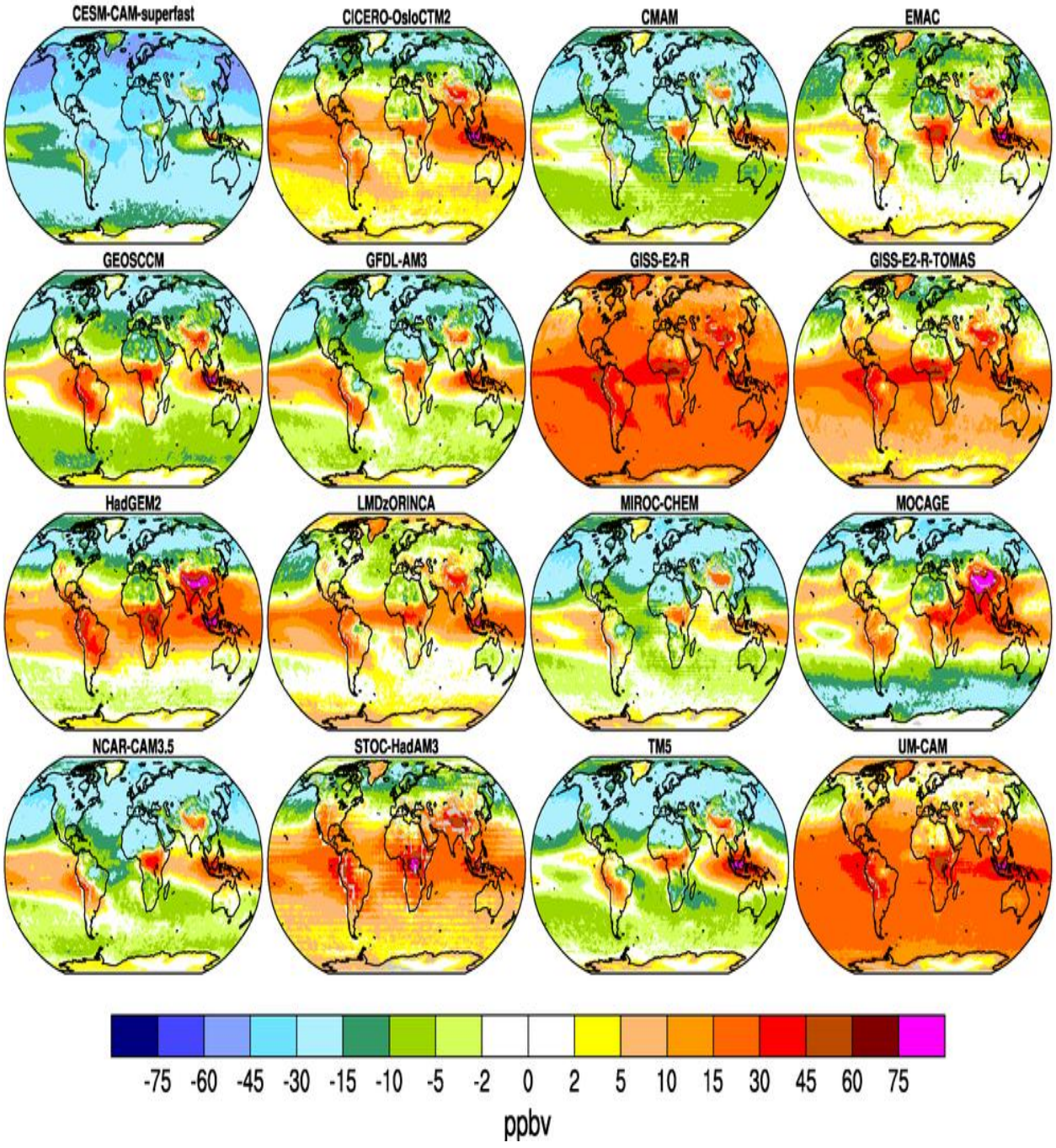

Figure S4. Percent change in regional tropospheric OH concentration for present day relative to the preindustrial simulated by each model. OH increases are shown in black and decreases are in red. Southern Hemisphere (SH), Northern Hemisphere (NH) and global mean (Glob) tropospheric OH changes are shown in the topmost row of each plot.

Figure S5. Same as in S4, but for percent changes in 2000 relative to 1980.